7

Feedback Control and Time-Optimal Control about Overhead Crane by Visual Servo and These Combination Control

Yasuo Yoshida
Chubu University
Japan

1. Introduction

Overhead cranes are broadly used in industry. However, undesirable load swing is often induced with transportation. Therefore, various researches about control of positioning and swing suppression of crane load have been made. On the other hand, a worker operates a crane skillfully by manual-operation in transportation. Hence, support system and automation of crane operation are expected from the viewpoint of safety and production efficiency.

Feedback, time-optimal and these combination controls by visual servo for practical use are described in this section. A visual servo device has the following two types. One type is installed separately from a crane and another type is installed on a trolley. Two problems related to the crane control will be discussed from here.

The first problem is feedback control by separate type of visual servo device. Separate type device is the case that the device cannot be installed on the crane. It has to track transportation movement and measure swing of the load. Base-line stereo which has parallel optical axes of two cameras uses parallax where tracked target point is not in the center of camera image and therefore, tracking control is difficult to succeed. Gaze controlled stereo vision device has the mechanism that an intersection point of two cameras optical axes always accords with the target and can catch the target point in the center of camera image. This stereo vision device is made and used it for experiments. Using camera image data and tracking controlled camera angles, crane load can be tracked and at the same time 3 dimensional position of the load can be got. By using these data, feedback control of positioning and swing suppression was applied to crane load in experiments.

The second problem is combination control of time optimal control and feedback control by installed type of visual servo device. Installed type device is not necessary to track transportation movement, then that is why 3D-camera fixed to trolley is used. This type device can measure displacements of both swing of the load and rope hoisting. Time optimal control is feed forward control. Trolley acceleration time for swing suppression control is set using exact natural period of load swing that is beforehand estimated. However, when with lack of information of actual rope length, position of center of gravity

or moment of inertia of crane load, it is often that an incorrect natural period of load swing is used, and swing is induced. Therefore, it is practical to use combination control of both time optimal control of transportation positioning and feedback control of swing suppression of the load and it was inspected by experiments.
In addition, when rope length changes while swing suppression control, feedback control needs variable control gains of nonlinear system. Then, the method that control digital gains can be redesigned by analog gains was developed and these variable digital gains were used in experiments.

2. Crane feedback control by gaze-controlled stereo vision installed separately from the crane

2.1 Dynamic model and control of overhead crane

An overhead crane model and a stereo vision installed separately from the crane are shown in Fig. 1. This system has five-degree-of-freedom (trolley x, y, rope length l, swing angle amplitude θ, swing direction angle ϕ). Stereovision has four-degree-of-freedom from θ_1 to θ_4.

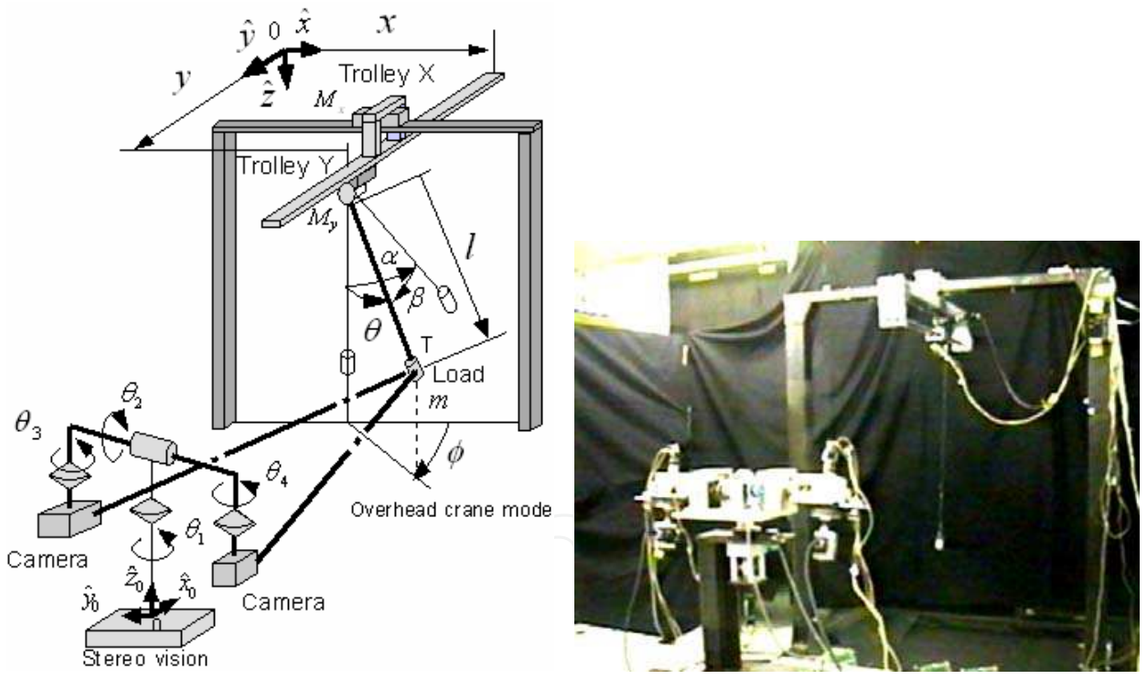

Fig. 1. Experimental model of overhead crane and stereo vision

Transportation and swing suppression are thought about the crane. The state equation associated with trolley displacement and swing angle is obtained using control input $\ddot{x} = u_x, \ddot{y} = u_y$,

$$\frac{d}{dt}\tilde{x} = A\tilde{x} + bu_x, \quad \frac{d}{dt}\tilde{y} = A\tilde{y} + bu \tag{1}$$

where

$$A=\begin{bmatrix}0 & 0 & 1 & 0\\ 0 & 0 & 0 & 1\\ 0 & 0 & 0 & 0\\ 0 & -\frac{g}{l} & 0 & -2\frac{\dot{l}}{l}\end{bmatrix},\quad b=\begin{bmatrix}0\\ 0\\ 1\\ -\frac{1}{l}\end{bmatrix},\quad \tilde{x}=\begin{bmatrix}x\\ \alpha\\ \dot{x}\\ \dot{\alpha}\end{bmatrix},\quad \tilde{y}=\begin{bmatrix}y\\ \beta\\ \dot{y}\\ \dot{\beta}\end{bmatrix}$$

Swing angles are supposed to be small values. Digital regulator where trolley displacements follow desired positions and swing angles decrease to zero value can be designed as,

$$u_{xk}=G_d\tilde{e}_{xk},\quad u_{yk}=G_d\tilde{e}_{yk}, \tag{2}$$

where

$$\tilde{e}_{xk}=\begin{bmatrix}x_d-x_k & -\alpha_k & -\dot{x}_k & -\dot{\alpha}_k\end{bmatrix}^T,\quad \tilde{e}_{yk}=\begin{bmatrix}y_d-y_k & -\beta_k & -\dot{y}_k & -\dot{\beta}_k\end{bmatrix}^T.$$

k = 1,2,… indicates time series with sampling time. From the closed loop relation between analog state and digital state that is redesigned to digitize the analog state, digital gain $G_d=\begin{bmatrix}k_{1d} & k_{2d} & k_{3d} & k_{4d}\end{bmatrix}$ can be obtained from analog gain G_a determined by pole assignment.

$$G_d=\frac{1}{2}\left(1+\frac{1}{2}G_aq\right)^{-1}G_a(I+p), \tag{3}$$

where

$$p=\left(I-\frac{T}{2}A\right)^{-1}\left(I+\frac{T}{2}A\right),\quad q=T\left(I-\frac{T}{2}A\right)^{-1}b.$$

Velocity of the trolley can be obtained from eq.(2) by integrating with sampling time.

2.2 Gaze-controlled stereo vision

Stereo vision is shown in Fig. 2 and camera (XV1000,Keyence Corp.) coordinates in Fig. 3. Camera image positions of moving point T indicated by camera coordinate 3c, 4c are expressed as,

$${}^{3c}P_T=\begin{bmatrix}0 & y_{3c} & z_{3c}\end{bmatrix}^T,\quad {}^{4c}P_T=\begin{bmatrix}0 & y_{4c} & z_{4c}\end{bmatrix}^T.$$

Therefore, point T indicated by target coordinate 3t, 4t can be expressed with image data,

$${}^{3t}P_T=\frac{a_1}{f}\begin{bmatrix}0 & y_{3c} & z_{3c}\end{bmatrix}^T,\quad {}^{4t}P_T=\frac{a_2}{f}\begin{bmatrix}0 & y_{4c} & z_{4c}\end{bmatrix}^T,$$

a_1, a_2 are distances from the lens center to the target-point along optical axes using $c_i\equiv\cos\theta_i$, $s_i\equiv\sin\theta_i$ ($for\ i=1\sim4$) and $c_{34}\equiv\cos(\theta_3-\theta_4)$, $s_{34}\equiv\sin(\theta_3-\theta_4)$,

$$a_1=\frac{2b\left(\frac{y_{4c}}{f}s_4-c_4\right)-r\left\{\frac{y_{4c}}{f}(1-c_{34})+s_{34}\right\}}{\frac{y_{3c}-y_{4c}}{f}c_{34}+\left(1+\frac{y_{3c}y_{4c}}{f^2}\right)s_{34}},\quad a_2=\frac{2b\left(\frac{y_{3c}}{f}s_3-c_3\right)+r\left\{\frac{y_{3c}}{f}(1-c_{34})-s_{34}\right\}}{\frac{y_{3c}-y_{4c}}{f}c_{34}+\left(1+\frac{y_{3c}y_{4c}}{f^2}\right)s_{34}} \tag{6}$$

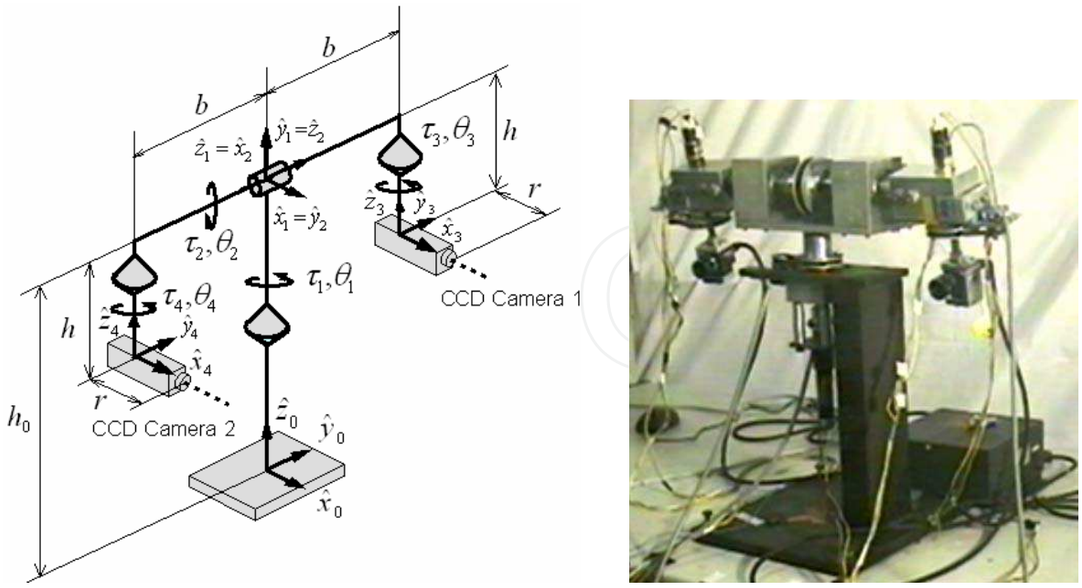

Fig. 2. Stereo vision installed separately from the crane

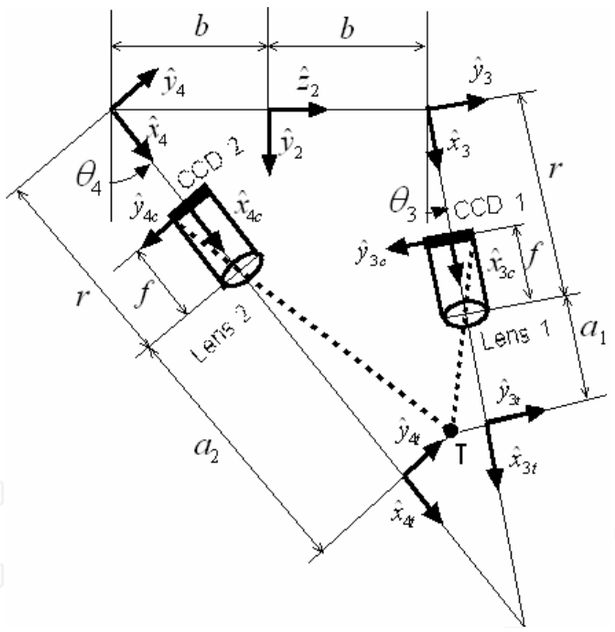

Fig. 3. Camera coordinates and optical axes

Positions by joint coordinate 3, 4 can be expressed,

$$ {}^3P_T \equiv \begin{bmatrix} {}^3x_T \\ {}^3y_T \\ {}^3z_T \end{bmatrix} = \begin{bmatrix} r + a_1 \\ (a_1/f)y_{3c} \\ (a_1/f)z_{3c} \end{bmatrix}, \quad {}^4P_T \equiv \begin{bmatrix} {}^4x_T \\ {}^4y_T \\ {}^4z_T \end{bmatrix} = \begin{bmatrix} r + a_2 \\ (a_2/f)y_{4c} \\ (a_2/f)z_{4c} \end{bmatrix} \tag{7} $$

From ${}^3P_T$, the position expressed with base coordinate 0 is given by,

$$ {}^0P_T \equiv \begin{bmatrix} {}^0x_T \\ {}^0y_T \\ {}^0z_T \end{bmatrix} = \begin{bmatrix} c_1 s_2 \left({}^3z_T - h \right) + c_1 c_2 \left(c_3 {}^3x_T - s_3 {}^3y_T \right) - s_1 \left(s_3 {}^3x_T + c_3 {}^3y_T + b \right) \\ s_1 s_2 \left({}^3z_T - h \right) + s_1 c_2 \left(c_3 {}^3x_T - s_3 {}^3y_T \right) + c_1 \left(s_3 {}^3x_T + c_3 {}^3y_T + b \right) \\ c_2 \left({}^3z_T - h \right) - s_2 \left(c_3 {}^3x_T - s_3 {}^3y_T \right) + h_0 \end{bmatrix} \tag{8} $$

Similary, the position of the target can be obtained from ${}^4P_T$. Fig. 4 (a) shows the gazing state where the target is on a point of intersection of optical axes of both cameras where the position is given by putting $y_{3c} = y_{4c} = 0$, $z_{3c} = z_{4c} = 0$ into eq.(7). Fig. 4 (b) shows the looking state of parallel optical axes of both cameras by putting $\theta_3 = \theta_4 = 0$ into eq.(7). Therefore, expressions of (6), (7) include not only gaze but also parallel stereo.

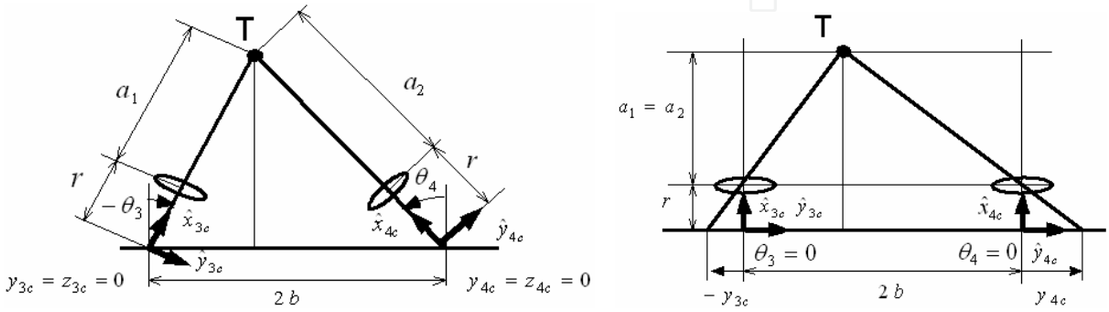

(a) Gazing the target (b) Looking using parallel optical axes

Fig. 4. Looking states using gaze and parallel optical axes of stereo cameras

We can see that the three-dimensional position of a crane load is the function with camera angles, image data, the focus distance and stereovision dimensions. It is gaze control that there is a moving point in the center of camera image, and tracking control that always catches a moving point to camera image.

When an intersection point of two cameras optical axes accords with a moving point, stereovision angles become target desired angles for the gaze/tracking control. Target desired angles as shown in Fig. 5 using measured position of eq.(8) are provided by inverse kinematics,

$$ \begin{aligned} \theta_{1d} &= A\tan 2\left({}^0y_T, {}^0z_T \right) \\ \theta_{2d} &= -\frac{\pi}{2} - A\tan 2\left({}^0z_T - h_0, \sqrt{\left({}^0x_T \right)^2 + \left({}^0y_T \right)^2} \right) \\ &\quad + A\tan 2\left(\sqrt{\left({}^0x_T \right)^2 + \left({}^0y_T \right)^2 + \left({}^0z_T - h_0 \right)^2 - h^2}, h \right), \\ \theta_{3d} &= -\theta_{4d} \\ \theta_{4d} &= A\tan 2\left(b, \sqrt{\left({}^0x_T \right)^2 + \left({}^0y_T \right)^2 + \left({}^0z_T - h_0 \right)^2 - h^2} \right) \end{aligned} $$

Digital controller by which the controlled angle θ_i follows the desired angle θ_{id} is given by,

$$ u_{ik} = k_{c1d}\left(\theta_{idk} - \theta_{ik} \right) - k_{c2d}\dot{\theta}_{ik} \quad (i = 1 \sim 4) \tag{10} $$

Manipulating velocities are obtained by integrating with sampling time.

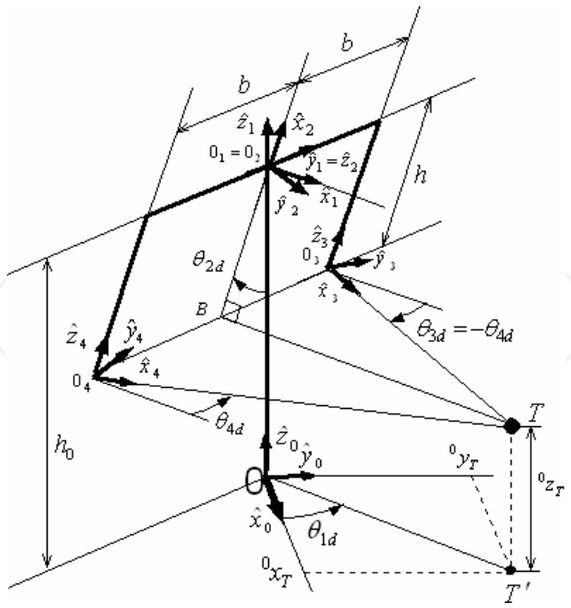

Fig. 5. Desired angles for gaze and tracking to control stereovision

2.3 Visual feedback control of overhead crane

Fig. 6 shows the block diagram of visual feedback control of overhead crane. Half of the upper part shows crane control, and half of the bottom shows stereo vision control.

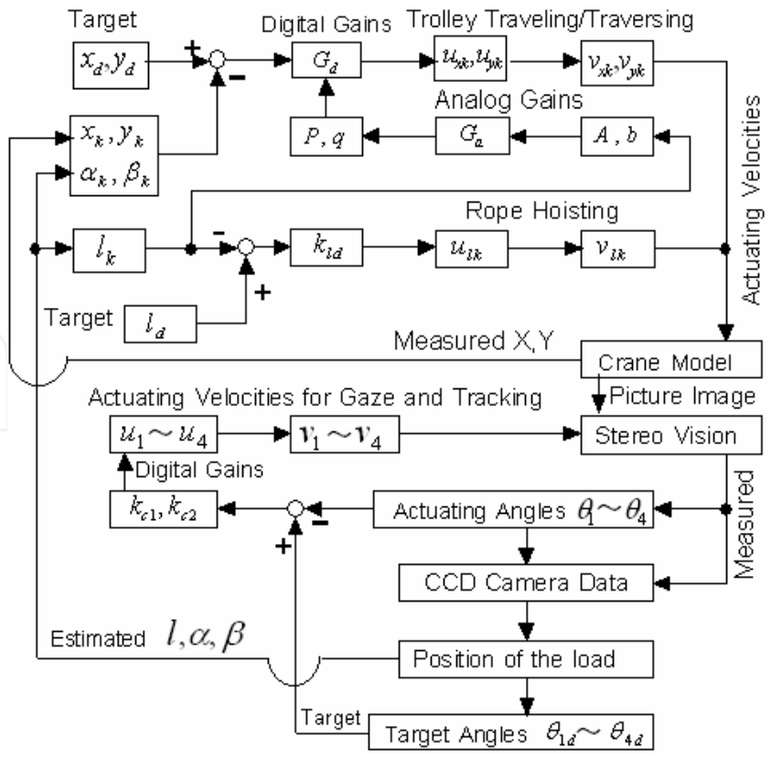

Fig. 6. Block diagram

Experimental results are shown from Fig. 7 to Fig. 11. In these figures, "with control" is defined that trolleys are controlled by visual feedback. Fig. 7 shows rope length. Hoisting the crane load is controlled where the rope length changes upward from initial length $1.25m$ to target length $0.8m$. Fig. 8 shows traveling and traversing transportation of trolley-X, Y. As for the controlled response, both of traveling of trolley-X and traversing of trolley-Y move to the target position $0.6m$ while doing swing suppression. Fig. 9 shows swing amplitude suppressed by visual feedback control though the rope length changes. Fig. 10 shows manipulating angles of stereo vision. The horizontal angle θ_1 changes largely to track the transportation of the load when trolleys are moving. And when the trolleys stay, it tracks the swing of the load, particularly large swing without control. The vertical angle θ_2 changes to track the hoisting of the load. Two camera angles θ_3, θ_4 change to gaze the load. Fig. 11 shows the changes of digital gains of trolley traveling and traversing. Gains change according to the rope length change of hosting of the load and the coefficient k_{2d} changes most, in proportion to swing angle that is sensitive for length.

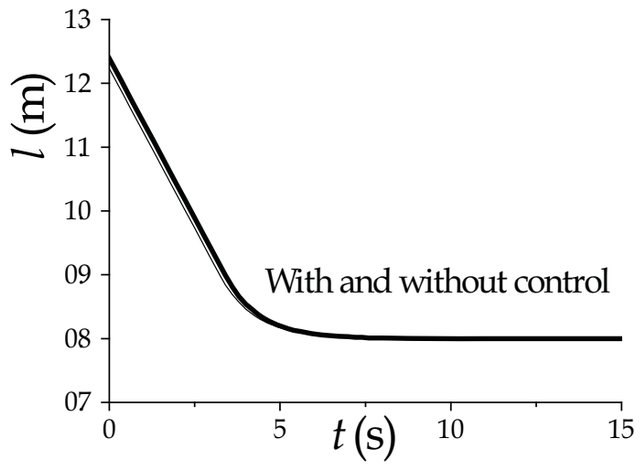

Fig. 7. Rope length with hoisting upward

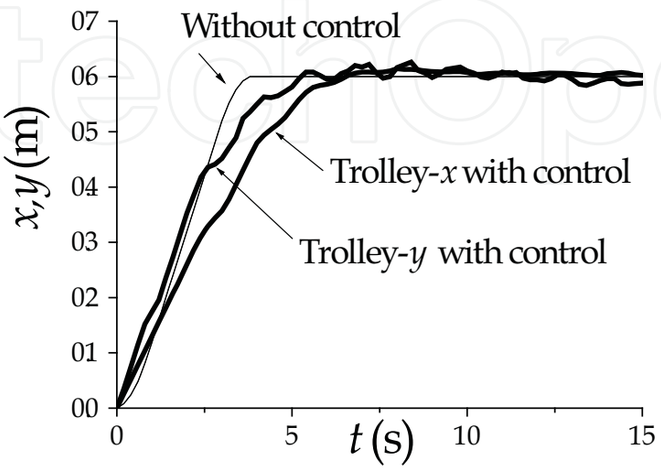

Fig. 8. Traveling and traversing transportation of trolley- X, Y

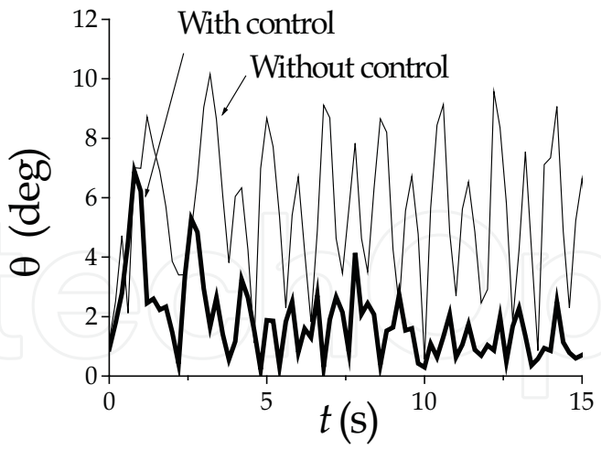

Fig. 9. Swing amplitude

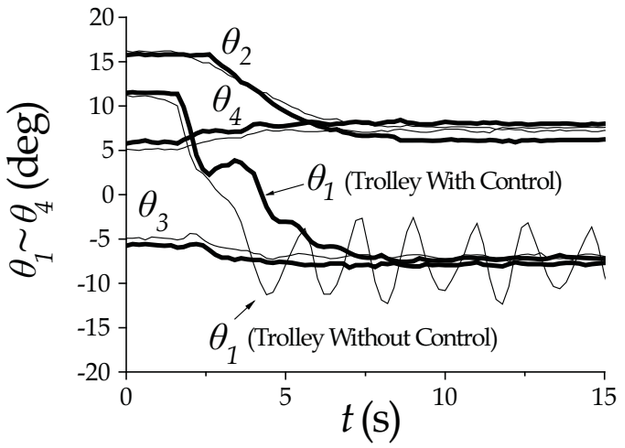

Fig. 10. Manipulating angles of stereo θvision

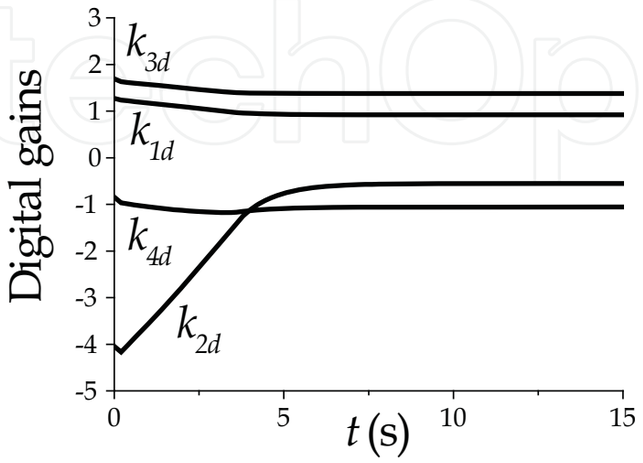

Fig. 11. Digital gains for crane control

3. Combination control of time optimal control and feedback control by 3D-camera installed on the trolley

3.1 Time optimal control as feed forward

Fig. 12 shows an overhead crane with 3D-camera (SR3000, CSEM Inc.) installed on the trolley and the marker on the crane load. Fig. 13 shows the crane load having constant rope length under the condition of trolley's constant acceleration u_0 .

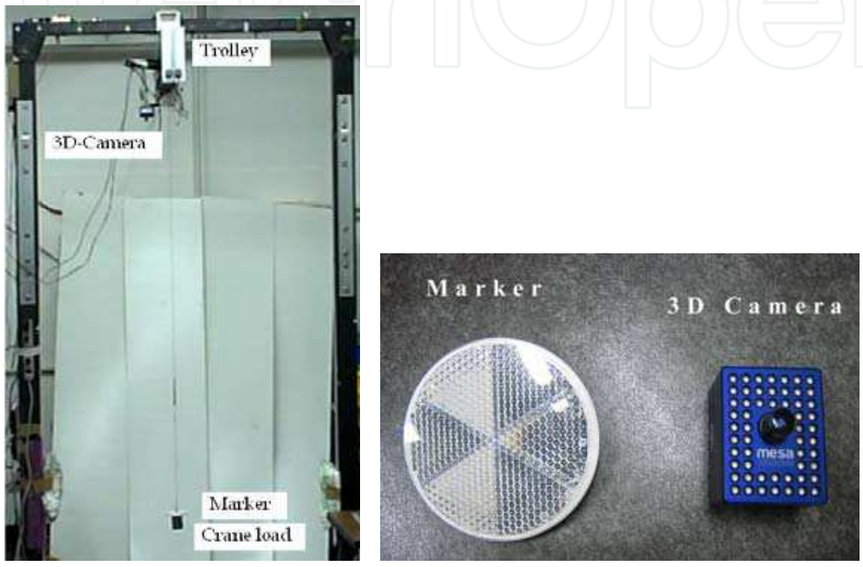

Fig. 12. Photograph of 3D-camera and marker

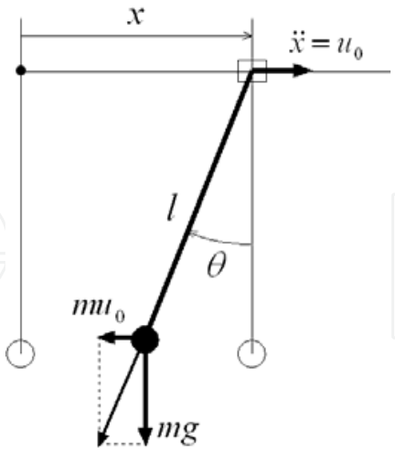

Fig. 13. Crane load under trolley's acceleration

The equations of motion is written as,

$$\ddot{\theta} + \omega^2 \theta = u_0 / l \tag{11}$$

where, $\omega = \sqrt{g/l}$ is natural circular frequency and $T = 2\pi/\omega$ is natural period.

Solution of eq.(11) is,

$$\theta = (1 - \cos \omega t) u_0 / g \tag{12}$$

When initial condition is $\theta(0) = \dot{\theta}(0) = 0$, the swing angle is maximum $\theta(T/2) = 2u_0/g$ at $T/2$ and $\theta(T) = \dot{\theta}(T) = 0$ at T. Therefore, when the trolley accelerates with u_0 from $t = 0$ to T, swing angle is zero after the time T. This is well known and we call this "synchronous control" here. To make the travelling time less than natural period T, there is time-optimal control where the acceleration u_0 and $-u_0$ are switched each other using the minimum principle. Fig. 14 shows time trajectory of feedforward control. Two of synchronous control and time-optimal control are indicated in phase plane of swing angle. Synchronous control moves around P-point of circle with radius $u_0/\ g$ in order O-A-C_1-B-O. Necessary time to move around the circle is natural period T. Time-optimal control moves in order O-A-C_2-B-O where A, B are switching points and center of arc A-C_2-B is Q-point. Necessary time T_{op} to move around is as follows,

$$T_{op} = 2T_\varsigma + T_\eta \ (\leq T), \tag{13}$$

where, $T_\varsigma = \varsigma/\omega, T_\eta = \eta/\omega,\ \eta = 2\tan^{-1}(\sin\varsigma/(2-\cos\varsigma))$.
Fig. 15 shows feedforward control of trolley. (a) is acceleration and (b) is velocity of trolley

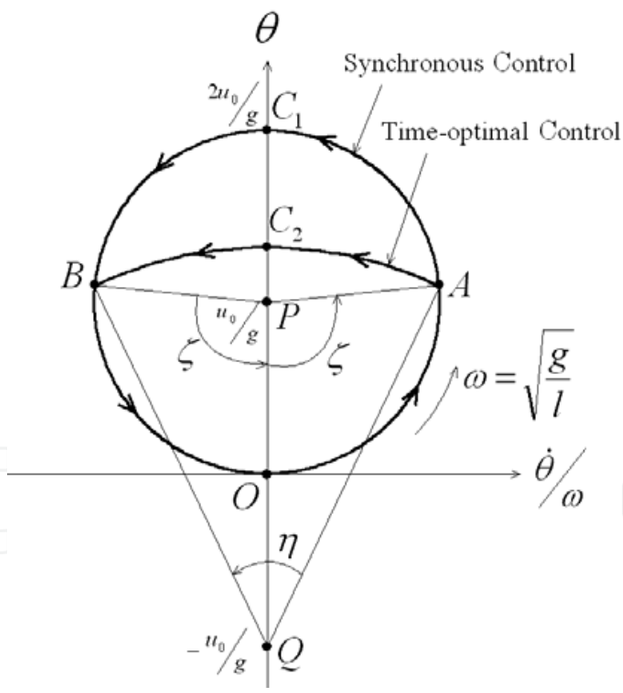

Fig. 14. Time trajectory of feed forward control

Fig. 16 shows time trajectory of feedforward control of trolley using false natural period $\omega_e = \sqrt{g/l_e}$ where l_e is error rope length. Synchronous control moves in order O-A-C_1-O-O_1 and necessary time becomes $(\omega/\omega_e)T$. Similarly, time-optimal control moves in order O-A-C_2-B-O_2 and necessary time becomes $(\omega/\omega_e)T_{op}$. As a result of these, residual swing vibration occurs as shown a circle around origin O-point with radius OO_1 or OO_2.

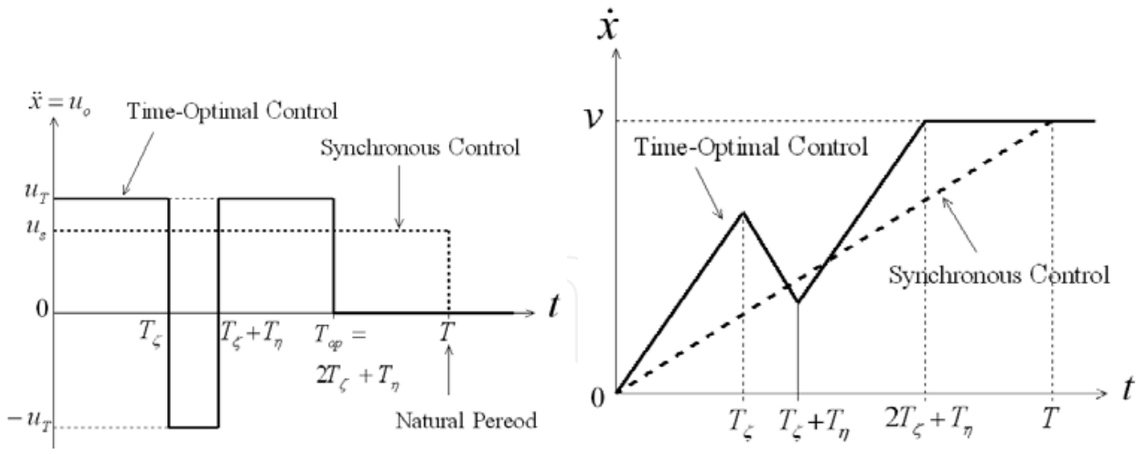

(a) Acceleration of trolley (b) Velocity of trolley

Fig. 15. Feed forward control of trolley

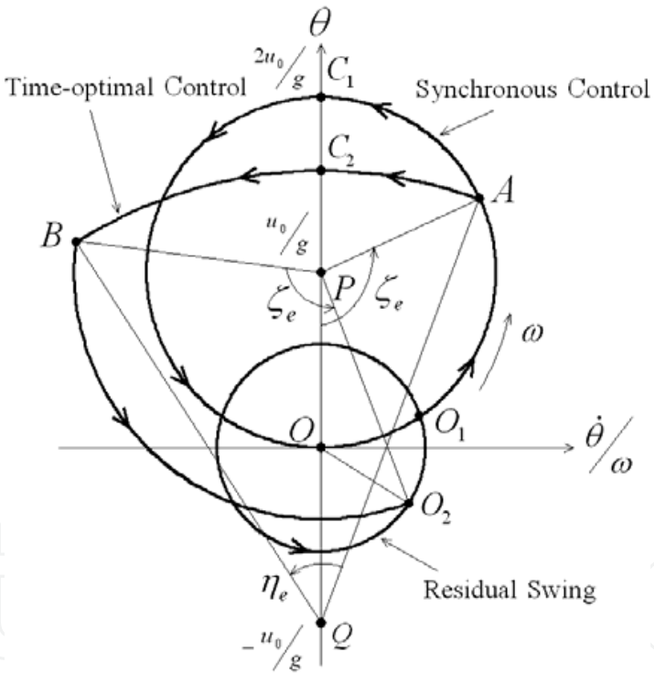

Fig. 16. Time trajectory of feed forward control using false natural period

3.2 Visual control experiments by 3D-camera

Three kinds of experiments using 3D-camera are done. These are experiment of feedback control, feed forward control and combination control.

(a) Visual feedback control experiment

Most of the same experiment as the visual feedback control by stereo vision was performed by 3D-camera. Fig. 17 shows rope length and trolley transportation. These are similar as results of Fig. 7 and Fig. 8 using stereo vision control.

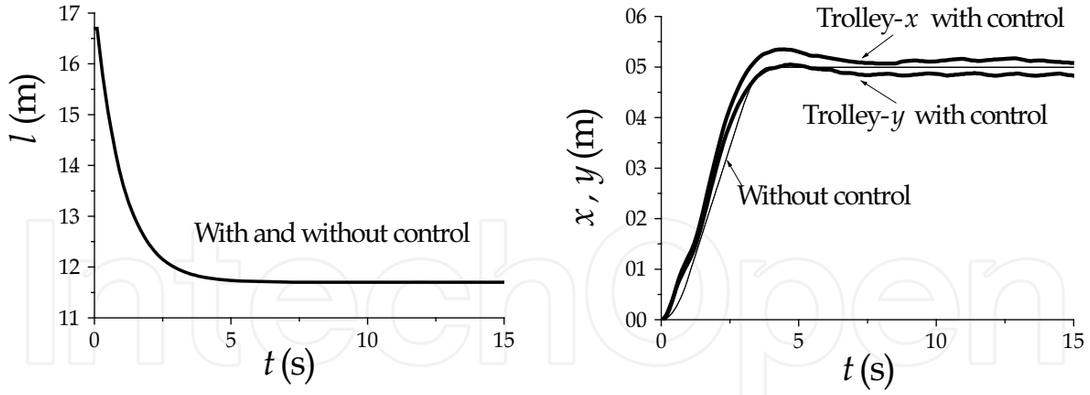

(a) Rope length with hoisting upward (b) Trolley transportation

Fig. 17. Rope length and trolley of visual feedback control using 3D-camera

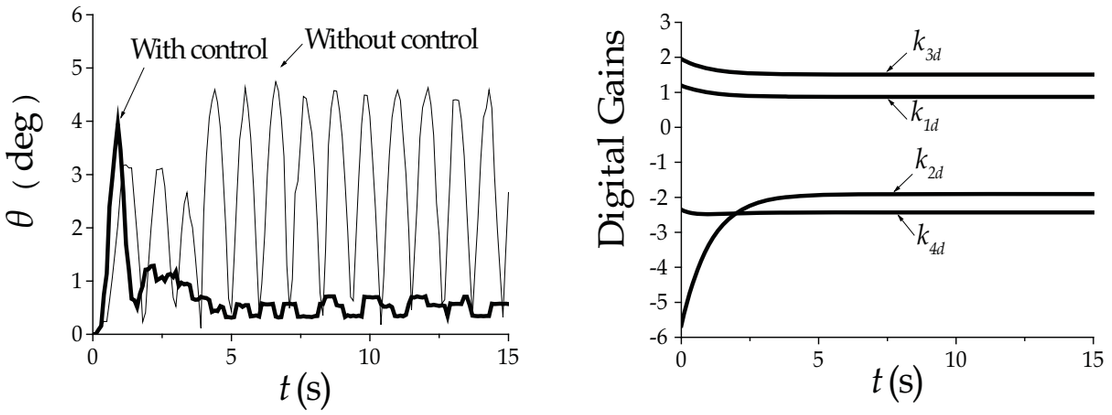

(a) Swing amplitude (b) Digital gains for crane control

Fig. 18. Swing amplitude and digital gains of visual feedback control using 3D-camera

Fig. 18 shows swing amplitude and digital gains for crane control. The swing vibration is suppressed using visual feedback by 3D-camera same as by stereo vision.

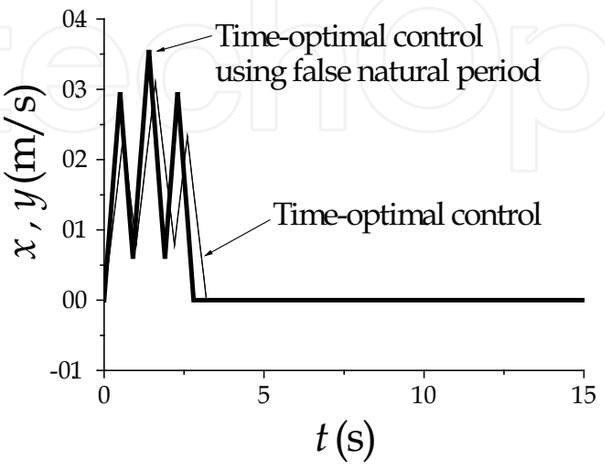

Fig. 19. Trolley's velocity

(b) Visual time-optimal control experiment

Experimental results of time-optimal control of the load suspended by rope length $l = 1.67m$ are from Fig. 19 to Fig. 21. Fig. 19 shows trolley's velocities of two patterns. One is time-optimal $T_\varsigma = 0.6s, T_\eta = 0.4s$ from correct natural period and another is error time $T_\varsigma = 0.5s, T_\eta = 0.4s$ using false natural period. Fig. 20 is the trolley's displacement controlled to the desire 0.5m. Fig. 21 is the swing amplitude. In the case of time-optimal control, the load swings with 4 deg amplitude until the time $2T_{op} = 3.2s$ and after that it stays without swing. In the case of the control using false natural period, the load swings with 5 deg until the time $2T_{op} = 2.8s$ and after that it's swing continues with 1.5 deg.

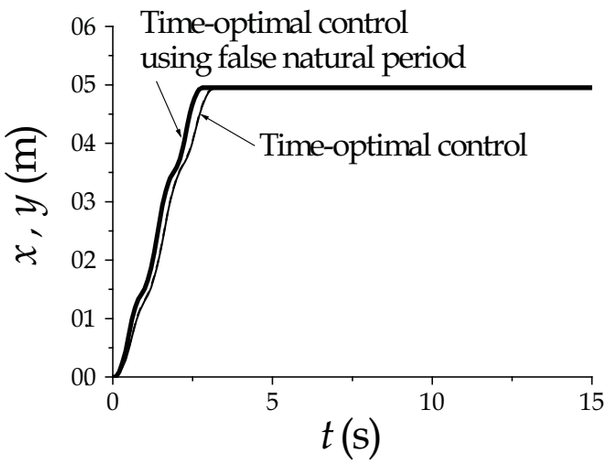

Fig. 20. Trolley transportation

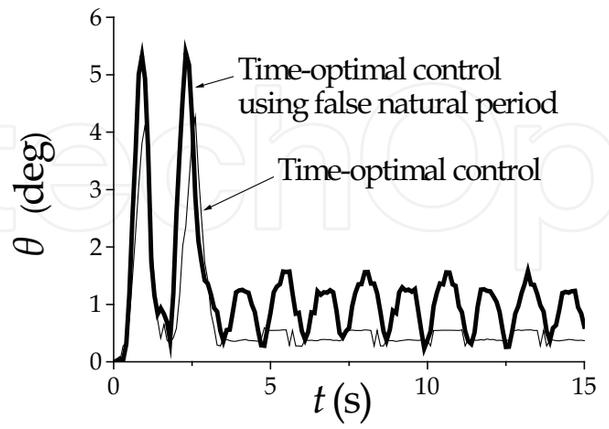

Fig. 21. Swing amplitude

(c) Combination control experiment

We tried the combination control that is the time-optimal feed forward control of transportation and the visual feedback control of swing suppression. Experimental results of

combination control are from Fig. 22 to Fig. 24. Fig. 22 shows trolley's velocities. In the first part, the time-optimal feedforward control with time $T_\varsigma = 0.5s, T_\eta = 0.4s$ using false natural period is used until $2T_{op} = 2.8s$ .Afterwards visual feedback control is used.

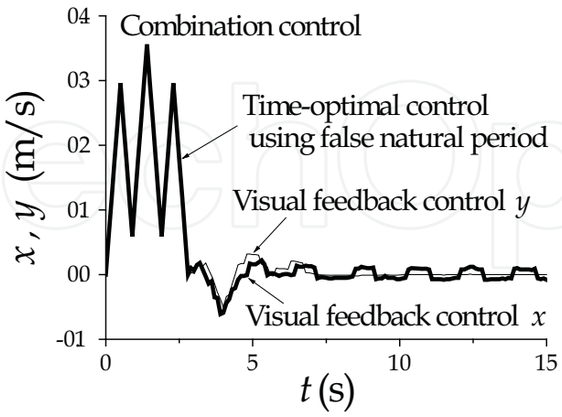

Fig. 22. Trolley's velocity

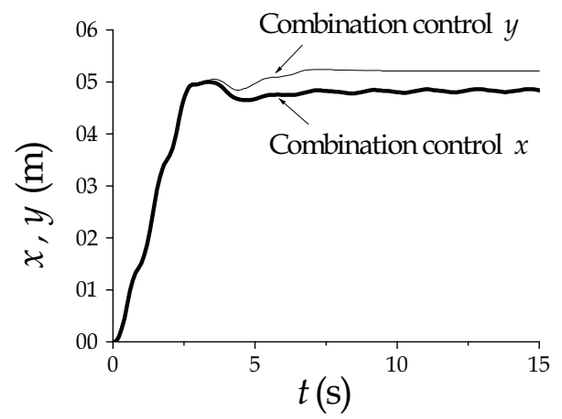

Fig. 23. Trolley transportation

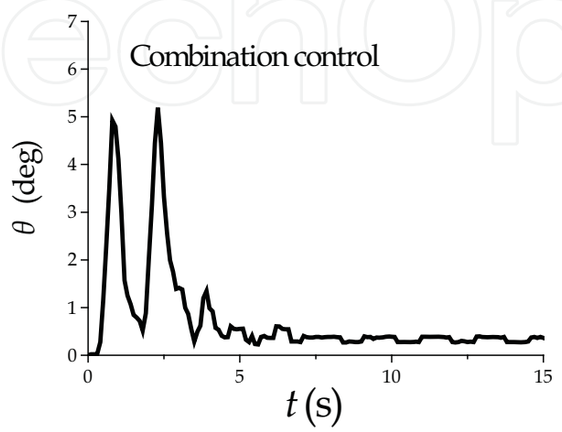

Fig. 24. Swing amplitude

Fig. 23 is the trolley's displacement controlled to the desire 0.5m. A little drift occurs in y direction. Fig. 24 is the swing amplitude. In this case, the load swings with 5 deg until the time $2T_{op} = 2.8s$, but after that it's swing decreased to zero by visual feedback control, different from Fig. 21.

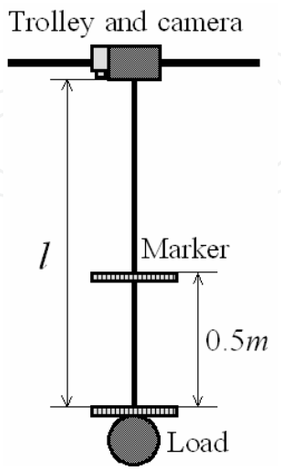

Fig. 25. Two different marker positions

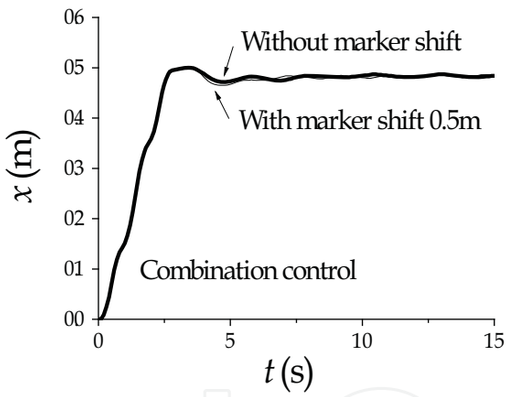

Fig. 26. Trolley transportation for arbitrary marker position

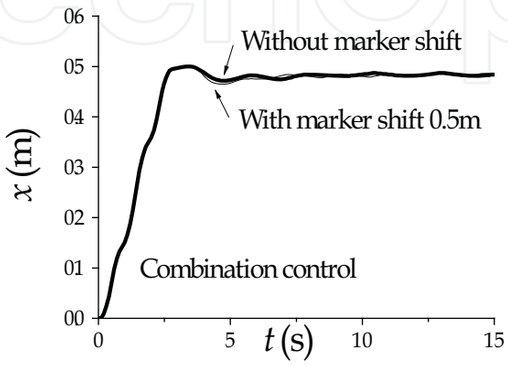

Fig. 27. Swing amplitude for arbitrary marker position

As for the load marker, it is realistic to install the marker on the crane hook or on the arbitrary position of the rope. Fig. 25 shows two different marker positions where one is installed on the load and another is located 0.5m upward. Fig. 26 and Fig. 27 are experiments using combination control for two different positions of load marker. No significant difference appeared in the response of trolley position and swing angle.

4. Conclusion

A trial stereovision device of separate type from the crane is manufactured and tried to control the overhead crane by vision feedback. Three-dimensional positions measurement and the control of tracking/gazing about the crane transportation load were carried out by the stereovision. Using measured visual three-dimensional load position, positioning and swing suppression control of the overhead crane was done. The experimental results of the overhead crane control by vision feedback showed that the used control system was effective. Next, combination control of time-optimal feedforward control for transportation and feedback control for swing suppression were carried out by a visual servo device using 3D-camera installed on the crane. The combination control is practical and effective for actual crane with various swing natural period. There is little influence which the installed location of a marker gives visual feedback control. In addition, when rope length changes while swing suppression control, feedback control needs variable control gains of nonlinear system. Then, the method that control digital gains can be redesigned by analog gains was developed and these variable digital gains were used in experiments.

5. References

Lee, H.H. (1998). Modeling and Control of a Three-Dimensional Overhead Crane, *ASME Journal of Dynamic Systems, Measurement, and Control,* Vol. 120, pp. 471-476.

Mita, T. & Kanai, T. (1979). Optimal Control of the Crane System Using the Maximum Speed of the Trolley (in Japanese with English abstracts), *Trans. of the Society of Instrumentation and Control Engineers, Japan,* Vol. 15, No.6, pp. 833-838.

Mostafa, K.A.F. & Ebeid, A.M. (1988). Nonlinear Modeling and Control of Overhead Crane Load Sway, *ASME Journal of Dynamic Systems, Measurement, and Control*, Vol. 110, pp. 266-271.

Papanikopoulos, N. P.; Khosla, P. K. & Kaneda, K. (1993). Visual Tracking of a Moving Target by a Camera Mounted on a Robot: A Combination of Control and Vision, *IEEE Trans. on Robotics and Automation*, Vol. 9, No. 1, pp. 14-35.

Yoshida, Y. (2004). Visual Feedback Control of a Three-Dimensional Overhead Crane, *Proceedings of ASME 7th Biennial Conf. on Engineering System Design and Analysis*, pp. 1-7, ISBN:0-7918-3741-6, Manchester, UK.

Yoshida, Y.; Hirano, M.; Tomida, T. & Teshima, H. (2005). Visual Feedback Control of Traveling Crane (in Japanese with English abstracts), *Trans. of the Society of Instrumentation and Control Engineers, Japan,* Vol. 41, No.6, pp. 527-532.

Yoshida, Y. & Tsuzuki, K. (2006). Visual Tracking and Control of a Moving Overhead Crane Load, *Proceedings of IEEE the 9'th Int'l Workshop on Advanced Motion Control*, pp. 630-635, ISBN:0-7803-9511-5, Istanbul, Turkey.

Yoshida, Y. & Tabata, H. (2008). Visual Feedback Control of an Overhead Crane and Its Combination with Time-Optimal Control, *Proceedings of the 2008 IEEE/ASME Int'l Conf. on Advanced Intelligent Mechatronics*, pp. 1114-1119, ISBN:978-1-4244-2495-5, Xi'an, China.

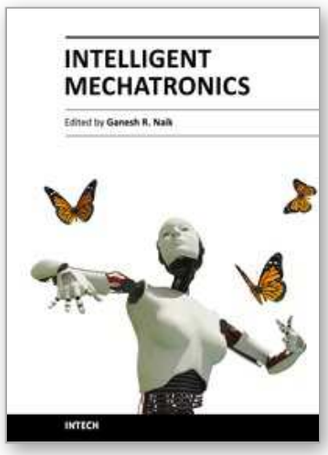

Intelligent Mechatronics

Edited by Prof. Ganesh Naik

ISBN 978-953-307-300-2
Hard cover, 248 pages
Publisher InTech
Published online 28, February, 2011
Published in print edition February, 2011

This book is intended for both mechanical and electronics engineers (researchers and graduate students) who wish to get some training in smart electronics devices embedded in mechanical systems. The book is partly a textbook and partly a monograph. It is a textbook as it provides a focused interdisciplinary experience for undergraduates that encompass important elements from traditional courses as well as contemporary developments in Mechtronics. It is simultaneously a monograph because it presents several new results and ideas and further developments and explanation of existing algorithms which are brought together and published in the book for the first time.

InTech Europe
University Campus STeP Ri
Slavka Krautzeka 83/A
51000 Rijeka, Croatia
Phone: +385 (51) 770 447
Fax: +385 (51) 686 166
www.intechopen.com

InTech China
Unit 405, Office Block, Hotel Equatorial Shanghai
No.65, Yan An Road (West), Shanghai, 200040, China
中国上海市延安西路65号上海国际贵都大饭店办公楼405单元
Phone: +86-21-62489820
Fax: +86-21-62489821

IntechOpen